World Journal of Nuclear Science and Technology, 2015, 5, 274-286
Published Online October 2015 in SciRes. http://www.scirp.org/journal/wjnst
http://dx.doi.org/10.4236/wjnst.2015.54027

Engineering of Fuel Plates on Uranium-Molybdenum Monolithic: Critical Issues

Jaime Lisboa[1*], Jorge Marin[1], Mario Barrera[1], Héctor Pesenti[2*]

[1]Departamento de Materiales Nucleares, Comisión Chilena de Energía Nuclear, CCHEN, Santiago, Chile
[2]Instituto de Materiales, Facultad de Ingeniería, Universidad Austral de Chile, Valdivia, Chile
Email: [*]jlisboa@cchen.cl, [*]hectorpesenti@uach.cl

Received 3 September 2015; accepted 25 October 2015; published 28 October 2015

Abstract

Engineering of nuclear fuels using monolithic plates of uranium-molybdenum and Al-6061 cladding is the current challenge for research and test reactors. The main drawback of the manufacture of monolithic nuclear fuel was analyzed using two surface coating methods: aluminum sputtering and transient liquid phase bonding (TLPB). Coating was done with a commercial alloy of Al-Si (R-4047). These techniques were used to improve the metallurgical bonding between the UMo and the cladding by rolling. Finally, design parameters and manufacture of UMo plate fuels were established. Mechanical tests were used to characterize the plates, resulting in UTS values of about 700 and 1000 MPa for the UMo alloys. These results are complemented with metrological analyses, X-Ray diffraction (XRD), thermal analyses, and metallography. X-rays and ultrasound scanners were used to monitor bonding and the co-rolling effects. These initial results show the main obstacles to the engineering development of UMo monolithic plate fuels with Al-6061 cladding, and these are discussed herein.

Keywords

Metallurgic Bonding, Co-Rolling, Monolithic UMo, Aluminum Alloy, Nuclear Fuel

1. Introduction

The terms of the international nuclear non-proliferation program have raised interest in the development of low-enriched uranium fuels (<20% ^{235}U) with fissile load densities similar to those of enriched fuels [1]. The alloy of uranium and molybdenum has shown itself to be a viable material for these purposes [1]-[3]. In fact, as

[*]Corresponding authors.

How to cite this paper: Lisboa, J., Marin, J., Barrera, M. and Pesenti, H. (2015) Engineering of Fuel Plates on Uranium-Molybdenum Monolithic: Critical Issues. *World Journal of Nuclear Science and Technology*, **5**, 274-286.
http://dx.doi.org/10.4236/wjnst.2015.54027

little as 7% - 10% Mo in the metallic U, this percent is enough to extend the domain of the γ-uranium phase stability, resulting in a much more stable phase for manufacture, irradiation, and a greater fissile load [4] [5]. In the manufacture of nuclear fuels, U-Mo is regularly dispersed on an aluminum matrix [6] [7]. Aluminum improves the uranium load by up to 8 gU/cm^3 and offers better heat transfer and greater performance in the "burning" of uranium than other common metals [8] [9]. However, the uranium load of aluminum is insufficient for high flux neutrons, and the formation of ternary reactions between Al-U-Mo is problematic, as the consequences for the fuel elements in the fission process are non-favorable [10]-[17]. One good solution for these obstacles is the development of U-Mo monolithic fuels [18]. This type of fuel improves the uranium load to approximately 16.0 gU/cm^3 for U7Mo alloys and reduces ternary transformations [16]. Studies of irradiated mini-plates have shown that this class of fuel satisfies the requirements of current reactors and the fuel elements also allow a good international qualification [17].

The main difficulties when manufacturing monolithic plates are the bonding of the UMo alloy plate to the aluminum cladding. This process usually occurs by deformation and so the metallurgical bonding between the metallic interfaces is very important. Therefore, a series of coating processes and materials have been proposed to improve the bonding process [17] [18]. Given these issues, several methodologies have been proposed to improve bonding: Hot Isostatic Pressing (HIP), the most widely used, most mini-monolithic plates have been produced using friction stir welding (FSW); the method of transient liquid phase bonding (TLPB) is one current methodology that has yet to been studied in depth [19] [20]. Considering the importance of metallurgical bonding, scaling the design of plate-type fuels, and the manufacture of monolithic fuels (which is significantly more complex than manufacturing disperse-type fuels) [19] [21], a faster progress in the engineering of the fuel elements based on monolithic UMo is crucial.

2. Experimental Procedure

2.1. Alloy Preparation

The initial natural uranium was cleaned chemically in a technical grade HNO_3 acid solution, placed in an alumina crucible and taken to fusion temperature under a controlled atmosphere in an induction oven. Subsequently, each sample was adjusted metallurgically with Mo and cast in a closed "pseudo-Dourville"-type ingot mold of conditioned graphite.

Later, the ingots that were obtained were reheated at 950˚C for 24 hours in a vacuum (10^{-5} Torr) and slowly cooled in a reducing argon atmosphere, in order to homogenize the microstructure of the ingots and to induce the transformation of the residual alpha phase, located on the grain boundary, in phase γ metastable stabilized with Mo [4] (**Table 1**).

2.2. Obtaining U and UMo Plates

These ingots were covered with an yttrium oxide and ethanol emulsion in order to avoid metallic adherence and interaction in the hot-rolling process. The alloys were isolated from the oxidizing environment through total encapsulation in low carbon steel that was sealed on the edges by TIG welding.

Table 1. Dimensions of the cast ingots.

N˚ casting	Casting name	Composition (%)		Ingot dimensions (mm)		
		U	Mo	Length	Width	Thickness
1	FUN-01	100	0	42.03	21.56	4.94
2	FUN-02	100	0	39.52	30.07	6.02
3	U10Mo	90	10	58.37	44.40	3.16
4	U10Mo	90	10	40.99	31.56	3.11
5	U7Mo-4	93	7	-	-	2.66
6	U7Mo-4	93	7	-	-	2.66

1) Hot Rolling

The observations of Sease *et al.* [21] were considered for the subsequent rolling process. These authors recommended intermediate reheating stages between the rolling steps to avoid the occurrence of hardening mechanisms caused by deformation in the UMo alloy, which would reduce the ductility of the material. In this phase, hot-rolling is done during reheating stages in a resistance oven; see **Table 2** for the process program.

Deformations of 80% to 96% total reduction were obtained in the steel-alloy-steel kit. During hot-rolling, these deformations were monitored metrologically during each fifth stage of reduction (**Table 3**).

2) Cold-Rolling

For cold-rolling, the surfaces of the U and UMo plates were cleaned to completely eliminate the yttrium oxide. The U and UMo plates were again encapsulated separately within stainless steel envelopes (grade 304). This protects the rollers and avoids any possible contamination by exogenous factors associated with the handling of the components. In this stage, the reductions do not surpass 3% in per rolling, for total reduction values of 7% to 14%.

2.3. Aluminum Sputtering and Co-Rolling

Finally, we used hot co-rolling to achieve a bond between the UMo plate and the alloy Al-6061 cladding. Prior to this technique, the adhesion of the interfaces was improved by covering each plate of the UMo alloy indistinctly with approximately 300 nm of metallic aluminum by sputtering. Later, the UMo alloy was encapsulated between two plates of Al-6061, as shown in **Figure 1**.

To avoid the allotropic transformation of the gamma phase (BCC) during the co-rolling process and the fusion of the Al-6061 cladding, a rolling temperature of 450˚C was used [22] [23]. In this process, each step reduced the thickness by 10% and, as in the process used to obtain the UMo plates, intermediate reheating was done between each stage.

2.4. TLPB and Co-Rolling

We proposed using the TLPB method to bond the U-7% Mo alloy plate with the alloy Al-6061 cladding, covering the UMo surface with aluminum and a commercial alloy of Al-Si Argenta TIG AL-194 (AWS R-4047). To compensate for the thickness of the cladding plates, one of the plates was reduced by the equivalent of the thickness of two plates of the Al-Si alloy (300 μm per plate) plus one plate of the UMo alloy (440 μm). Finally, we put the kit of materials together as shown in **Figure 2**.

Table 2. Program of hot-rolling process according to Sease *et al.* [21].

Material	Heating temp. (˚C)	Time (h)	1st rolling stage		2nd rolling stage	Reheating times per step (min)
			Reduction per step (%)	Nº. of steps	Reduction per step (%)	
Uranium	630					
U7Mo-4	680	1	5	4	10	10
U10Mo	680					

Table 3. Dimensions of hot-rolled samples.

Alloy	T (˚C)	Reduction (%)	Thickness (mm)	Width (mm)	Length (mm)
FUN-01[a]	630	95.93	0.201	46	501
FUN-02[b]	630	94.52	0.330	33	676
U7Mo[a]	680	84.97	0.475	61	283
U7Mo-4[b]	680	87.07	0.402	33	265
U10Mo[a]	680	81.65	0.508	-	-
U10Mo-4[b]	680	81.39	0.490	-	-

[a]Casting direction; [b]Transverse casting direction.

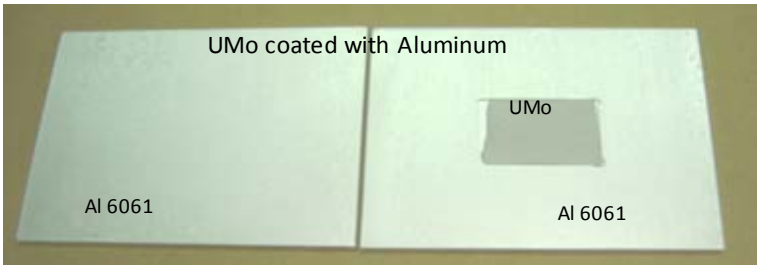

Figure 1. Assembly of one nuclear fuel plate: UMo alloy was coating with aluminum by sputtering.

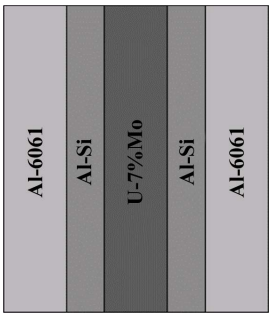

Figure 2. Graphical representation illustrating the assembly of one plate.

Two assays were carried out to study the bonding of the U7Mo-Al6061 systems. The first consisted of two stages: a TLPB treatment followed by the co-rolling of the set (**Figure 2**). For the second assay, co-rolling was simultaneous with a TLPB treatment.

3. Results and Discussion

Metal adhesion did not occur when the ingots of metallic uranium and UMo alloys were encapsulated in low carbon steel plates and yttrium oxide was incorporated. This allowed noticeably positive hot-rolling (**Figure 3**).

1) Metallic Uranium

In general terms, the production of uranium foil by rolling methodology was carried out successfully. Regarding to the results obtained, using the same procedures, in Indonesia and ANL-USA, the uranium foil manufactured at CCHEN had very lower thickness, even compared with the values reported by J. Taub *et al.* [24]. These foils present very acceptable surface quality and very regular thicknesses. Due to this, just few cold rolling passes will be enough to obtain uranium foils under specifications in terms of roughness and surface quality. The surface quality of foils fabricated at CCHEN does not exhibit surface defects as the reported by Kim *et al.* [25].

The X-ray films revealed that, during hot-rolling, the metallic uranium in the FUN-01 ingot (rolled lengthwise, in the casting direction) behaved better when elongated, allowing reductions exceeding 95%. The reductions of the FUN-02 plate (rolled transverse to the casting direction), however, were lower than expected (**Table 2**). Therefore, we can say that the dendritic structure of the casting is exclusively dependent on the texture. According to the mechanical tests, the FUN-01 plate presented an ultimate strength about to 392 MPa, whereas the FUN-02 plate presented an ultimate strength about to 479 MPa, both strength values are lower than the reported for metal uranium rolled and annealed [24]. The most interesting of these results was the maximum lengthening of the FUN-01 plate by rolling; this obtained an elongation of 2394%, whereas FUN-02 reached only 1711% elongation (**Figure 4**).

These results show that the maximum performance that can be obtained from metallic uranium in the rolling process is significantly affected by the direction of casting with respect to that of rolling. Whereas rolling transverse to the casting direction increases strength to deformation, rolling in the casting direction results in the maximum stretching of the plates.

2) Uranium-Molybdenum Alloys

(a) (b)

Figure 3. Fuel plates after hot-rolling: (a) Natural uranium, and (b) UMo alloy.

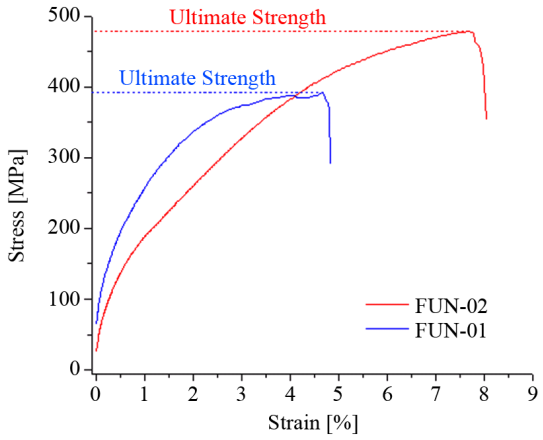

Figure 4. Tensile test diagram of uranium foil.

The main result of this study was the technological development of UMo monolithic plates having a thickness of 400 to 500 μm through hot-rolling, with reductions of 85% to 87%, a clean surface, and without apparent rugosity. This confirms that the encapsulating technique reported by Idaho National Laboratory INL [26] [27] is apt for obtaining thin plates of UMo alloys (**Table 4**).

Figure 5 shows the heightened tensile strength of the cold-rolled alloys. According to the tensile tests, the ultimate tensile strength in hot-rolling of the U7Mo alloy was 713 MPa, whereas the ultimate tensile strength in cold-rolling step was slightly higher (764 MPa), with a 10% reduction in thickness. On the other hand, the ultimate tensile strength of the U10Mo alloy was 972 MPa in hot-rolling and 1092 MPa in cold-rolling, with a reduction of 12.32% in thickness. Evidently, the greater molybdenum content of the U10Mo alloy is reflected in greater tensile strength.

Observations using DRX reveal that UMo alloys of castings present the *Im*3*m* (229) crystal structure of the γ phase of uranium [28], prevalently oriented to the plane (110) (**Figure 6(a)**). The U10Mo-4 sample presents a slight increment in the amplitude at the base of the diffraction peaks, which could be due to that fact that it presents more structural inhomogeneities due to different thermal gradients during the cooling process of the casting.

The hot-rolling process was performed according to the casting direction in two distinct samples, as follows: U10Mo, casting direction and U10Mo-4, transverse casting direction. The hot-rolling of the sample U10Mo1 produced a rotation of the crystal distribution of the plane (110) to a new orientation of the plane (211) and (200), as observed in **Figure 6(b)**.

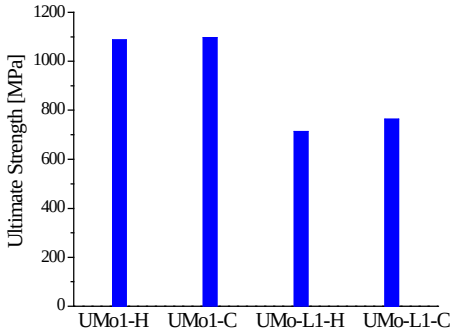

Figure 5. Comparison of ultimate strength in UMo alloys: U7Mo (UMo1) and U10Mo (UMo) in hot (H) and cold (C) rolling.

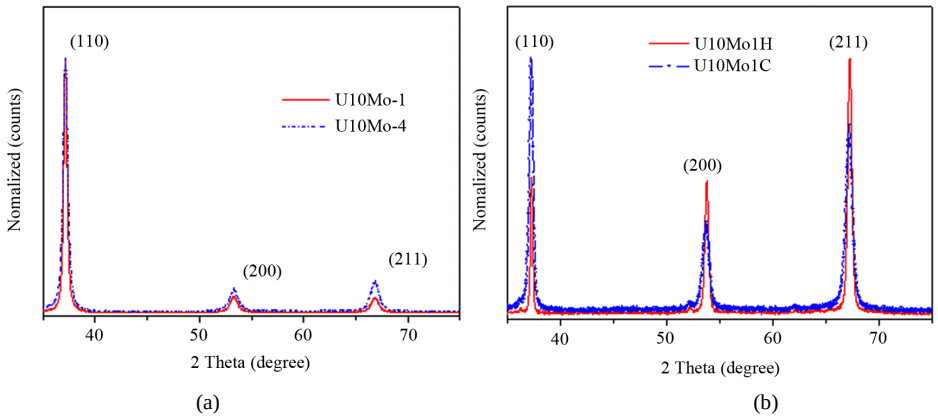

Figure 6. XDR pattern profile comparison of the casting of the U10Mo alloy samples (left); hot-rolling of the U10Mo1H alloy and cold-rolling of the U10Mo1C alloy samples (right).

Table 4. Summary of results obtained in the cold-rolling stage.

Alloy	Reduction (%)	Thickness (mm)	Initial length (mm)	Final length (mm)
U7Mo[a]	12.32	0.417	100.87	113.63
U7Mo-4[b]	7.24	0.373	100.92	106.88
U10Mo	10.00	0.457	100.70	111.25
U10Mo-4	14.37	0.420	100.34	116.93

[a]Casting direction; [b]Transverse casting direction.

The subsequent cold-rolling process of the alloy U10Mo resulted in a reduction in thickness of around 12.32%. Again, this produced an important change in the crystal distribution, returning it to the distribution of orientation of the planes (110) and sustaining the planes (211) (**Figure 7**). Hot-rolling over the ingot of the U10Mo-4 alloy also produced a slight rotation of the crystal distribution of the planes (110) towards the planes (200) and (211).

The cold-rolling of alloy U10Mo-4, with a reduction of 7.24%, induced the reorientation of the crystal dispositions to the planes (110) as well as the reduction of the intensities of the planes (200) and (211); similar phenomena were produced in the alloy U10Mo-1. Using DRX, we can deduce that hot-rolling the alloy U-Mo in the casting direction favored the crystalline planes (110) and (211) and that hot-rolling in the transverse casting direction favored the texture of the plane (211). The literature reports that metallic materials with the crystal structure BCC tend to form a fibrous texture, particularly the alpha type [29] [30], and tend to maintain orientations from (110) to (211) in the rolling process when no precipitation of some other compound is produced [31] [32], similar to what could occur with this class of alloy.

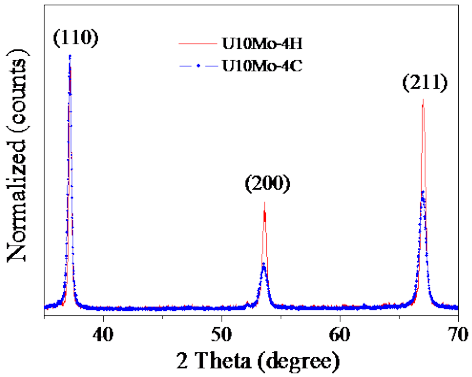

Figure 7. XDR pattern profile comparison of the hot-rolling and cold-rolling of the U10Mo-4 Alloy samples.

In terms of texture, the distribution of orientation of the polycrystals in the alloy U10Mo of the thin plates does not change significantly after hot- and cold-rolling. Rather, the stability of the alloy favors a displacement of the crystal planes between (110) and (211). Likewise, the parameters of the crystal cell were optimized using the Rietveld method (Topas v3, Bruker AXS), obtaining respective values of 3.430 (U10Mo) and 3.454 Å (U10Mo-4). Hot-rolling resulted in crystal cells with a value of 3.420Å (both castings) and cold-rolling gave values of 3.427 (U10Mo) and 3.421 Å (U10Mo-4). The difference in values from the casting of the material to the last process could be due to the accommodation of the crystal dispositions in the hot-rolling process and finally, a slight tension in the superficial crystal lattice caused by cold-rolling.

3) Aluminum Spputering and Co-Rolling the U-Mo Alloy

The co-rolling technique was done using plates of the alloy U7Mo. These plates were prepared in order to obtain good surface coverage, that is, a substrate of around 300 nm of pure aluminum through the process of sputtering. Previously, the Al-6061 cladding were pickling to assure a clean surface and to favor effective metallurgical adhesion in the co-rolling processes (**Figure 1**). The co-rolling process was initiated by reheating the kit at 450˚C for 1 hour and, later, reductions of 10% were obtained with each step of hot-rolling. The X-ray analysis of the co-rolled kits revealed multiple fractures in the UMo plates within cladding (**Figure 8**).

These results are inappropriate for the technological objectives of plate fuels mainly because of two factors in the process: 1) the low ratio of plastic deformation of the UMo to that of the cladding (Al alloy) and 2) the high sensitivity to the speed of deformation of the UMo with respect to the cladding materials (Al alloy). On the other hand, the lack of bonding resulted in swelling, and the occluded air caused the volume to increase at the process temperature. To obtain a better performance of the formability of the U-Mo alloy, it may be necessary to work at higher temperatures that exceed the isothermal transformation curves of the UMo alloy, thereby avoiding the transformation of the metastable gamma phase. According to the reported by Clark *et al.* [18], a thin layer of other element between the surface of UMo foil and the structural aluminium cladding (Zr at INL and Al at CCHEN) may produce reaction products, which induces an embrittlement in the alloy during the fuel plate manufacturing. In the case of this work, is more critical due to the thermomechanic process applied for the bonding of the fuel plate components.

The ultrasound sweep allowed us to confirm the lack of bonding of the fuel plates. **Figure 9** clearly shows all the defects from this part of the study related to this technique. The amplitudes are graphically expressed in relation to the metallic interaction. From another point of view, the substrate of 300 nm of Al incorporated over the surface of the U7Mo alloy was apparently insufficient for making optimum contact during the co-rolling process.

4) TLPB Process

For the TLPB study, we prepared multi-plate assemblages as indicated in **Figure 2**. Moreover, to assure contact between the multi-plates, we placed four rivets in the periphery of the fuel material. Finally, the entire contour was sealed using unsupported TIG welding around all the edges. **Figure 10** shows the assembled, welded set and the location of the UMo plate and the alloy Al-Si plates within the cavity.

The thermal analysis was done to verify the main points of thermodynamic change and the interaction of the

Figure 8. Mini-plates by hot- and cold-rolling: X-ray radiography.

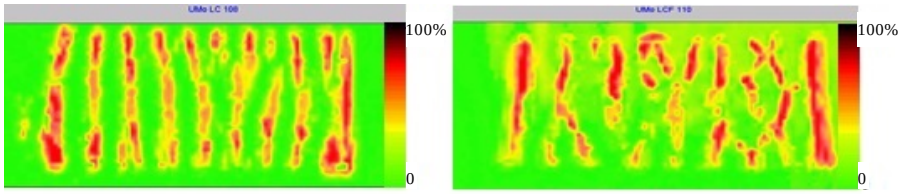

Figure 9. Ultrasound C-scan image, red areas show metallic adhesion and yellow areas the lack thereof.

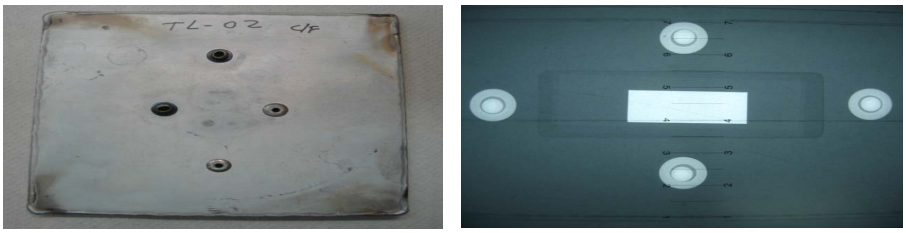

Figure 10. TL-02 assembly: assembled and welded set and X-ray image; the square shows the cavity in which the U7Mo meat alloy is found.

alloys under the effect of the high temperatures. In the Differential Scanning Calorimetry analysis (DSC) (**Figure 11**), we observed an endothermic reaction around 582˚C that corresponded to the fusion of the alloy Al-Si. Likewise, a second endothermic reaction around 640˚C corresponded to the fusion of the Al-6061. Subsequent increments of the temperature revealed accelerated oxidation of the metallic elements.

Given a known fusion temperature for the alloy Al-Si, the sets were subjected to gradual heating in a resistance oven under conditions similar to those used in the DSC analysis. This formed a transient liquid of the alloy Al-Si between the plates. **Table 5** shows the temperatures, times, and final state of the TLPB process.

Once the TLPB treatment was performed, the sets were analyzed through Ultrasonic Scanning conducted by immersion. The images in **Figure 12** and **Figure 13** indicate that the TLPB process applied to the sets TL-01 and TL-02 results successful, it mean that the interfaces Al-6061/Al-Si/U7Mo were bonded. Nevertheless, this cohesion was produced on the opposite face to the machined Al-6061 cladding, as is shown in the **Figure 13(b)**. Besides, during the co-rolling process, the set TL-01, with a total reduction applied of 62%, exhibits fragmentation of U7Mo foil, shown in the cross section and radiography of **Figure 12**.

The results of the six-hour TLPB treatment of sets TL-03 and TL-04 were not good. The set TL-03 presented only partial bonding of the interfaces and the set TL-04 did not bond (**Figure 14**, **Figure 15**). The fact that these two kits did not bond is apparently due to the fact that the alloy Al-Si remained in a liquid state for a long time and propagated over the surface, exiting the reduced area of the cladding Al-6061. In the co-rolling stage, the sets were worked at a temperature of 570˚C in order to assure the gamma phase during the hot-rolling process.

Table 6 summarizes the main results of the co-rolling stage. These were done with intermediate reheating between each reduction stage, as were the earlier hot-rolling processes.

During the fourth hot-rolling step of the co-rolling process of the TL-01 set, corresponding to a 62% total reduction, the U7Mo plate cracked, as can be seen in **Figure 12**. This behavior, as well as the large reduction applied, can be attributed to the fact that, before being subjected to rolling, the rivets were removed from this set, which could have affected the control of the oxidation of the set. In the set TL-03, during the third hot-rolling

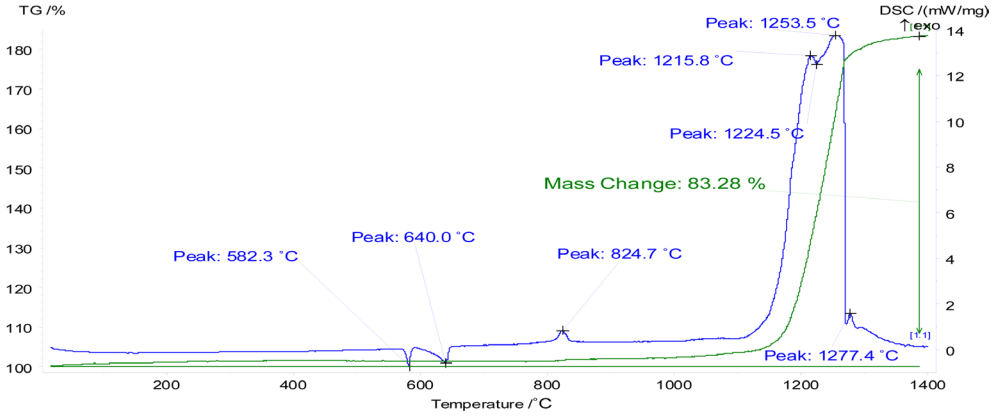

Figure 11. Thermal analysis curves of the ternary system Al-6061/Al-Si/U7Mo.

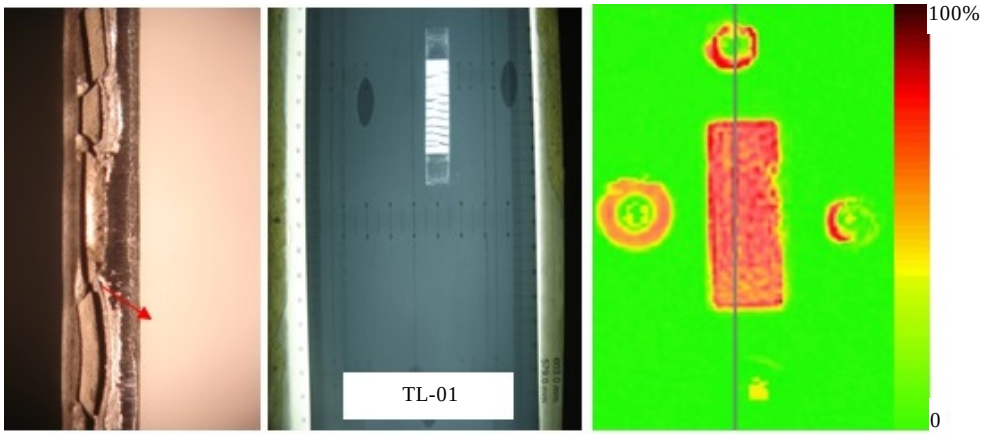

Figure 12. Illustration of TL-01 assembly: left; Metallographic image: lateral section of the fuel plate, showing multiple fractures, center; X-ray of the TL-01 set: frontal view of the multiple fractures and right; ultrasound C-scan image, red areas show metallic adhesion and yellow areas the lack thereof.

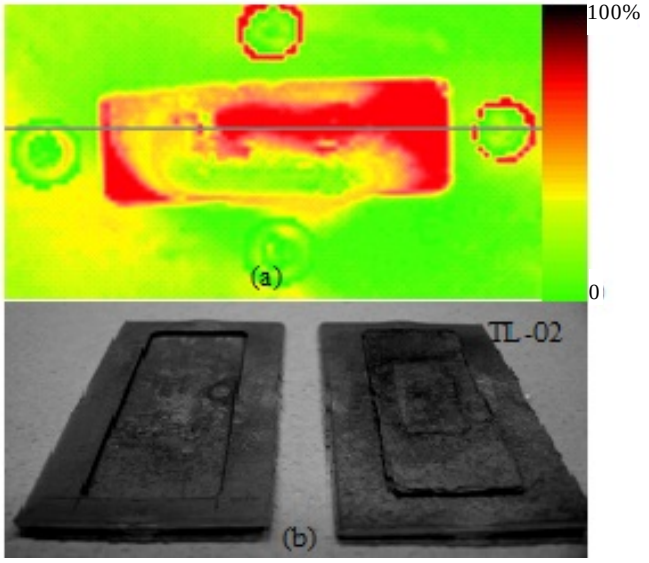

Figure 13. Images representation of TL-02: (a) C-scan image: red areas show metallic adhesion and yellow areas the lack thereof (b) TL-02 set picture.

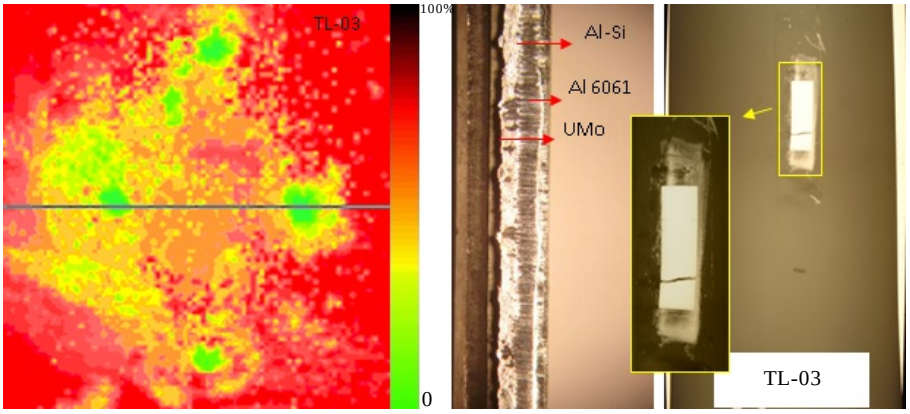

Figure 14. Illustration of TL-03 assembly: Left: ultrasound C-scan image, red areas show metallic adhesion and yellow areas the lack thereof. Center: metallographic image, lateral section of the fuel plate and right: X-ray of the TL-03 set, frontal view showing one fractures.

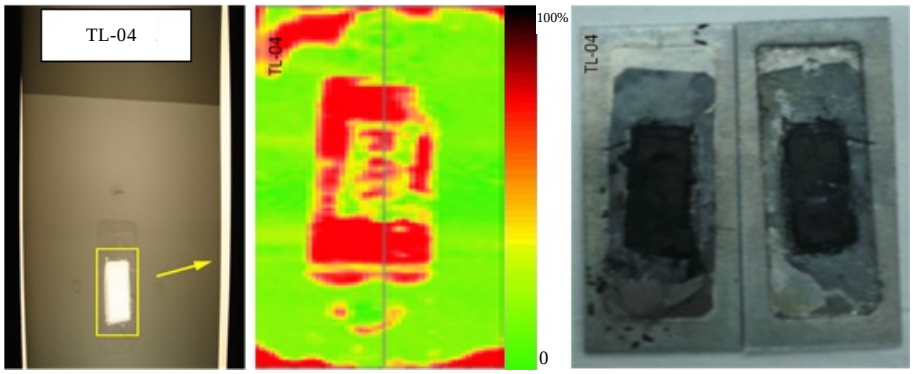

Figure 15. TL-04 set: left: X-ray image, center: ultrasound C-scan, and right: photography of the open set.

Table 5. Treatment conditions of the process.

Set	Process	Deposit		Plate (μm)	Time (h)	T (˚C)	Final state
		Alloy	Thickness (μm)				
LH-108	Sputtering	Al	0.150	330	-----	-----	-----
LHC-110	Sputtering	Al	0.300	330	-----	-----	-----
TL-01	TLPB	Al-Si	313	440	2	590	Bonded
TL-02	TLPB	Al-Si	289	440	2	600	Bonded
TL-03	TLPB	Al-Si	321	433	6	590	Partially bonded
TL-04	TLPB	Al-Si	316	433	6	590	Not bonded
TL-05	TLPB	Al-Si	314	478	-----	570	-----
TL-06	TLPB	Al-Si	312	478	-----	570	-----

step (47% total reduction), the cladding broke at the ends of the contact zone between the two alloys (Al-Si and Al-6061). The X-ray in **Figure 14** shows a transversal fracture of the U7Mo plate and small cracks at the lower edge of the plate. The micrograph shows good bonding between the system components. In set TL-04, during the second hot-rolling step (17% total reduction), the cladding was broken at the ends of the contact zone between the two alloys (Al-Si and Al-6061) and in the contact zone of U7Mo and Al-Si. However, unlike sets TL-01 and TL-03, this kit does not present cracking in the U7Mo lamina as was found in the X-ray. The ultrasound image

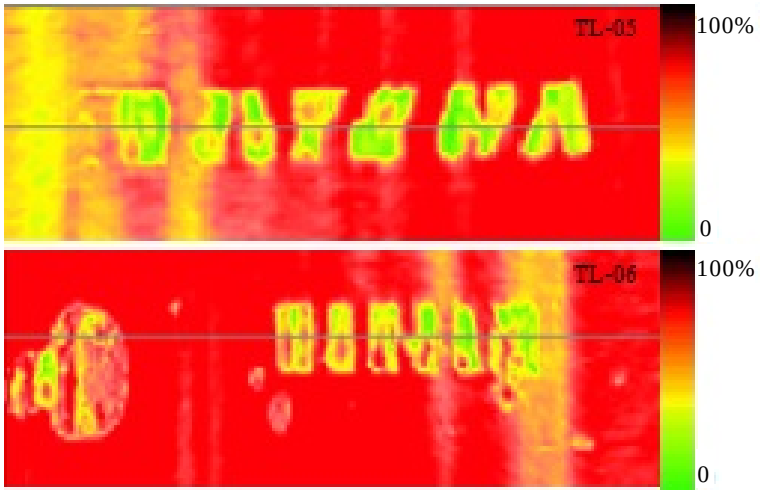

Figure 16. TL-05 and TL-06 sets: Ultrasound image C-scan and B-scan of sets TL-05 and TL-06.

Table 6. Treatment conditions of the process.

Set	Deposit	Co-rolling (˚C)	Reduction (%)	Final stage
LH-108	Al	450	50	Not bonded
LHC-110	Al	450	50	Not bonded
TL-01	Al-Si	570	62	Not bonded
TL-02	Al-Si	-----	-----	-----
TL-03	Al-Si	570	47	Partially bonded
TL-04	Al-Si	570	17	Partiallybonded
TL-05	Al-Si	570	68	Partially bonded
TL-06	Al-Si	570	68	Partially bonded

shows partial bonding in this kit after the co-rolling step.

Sets TL-05 and TL-06 were subjected to simultaneous processes of TLPB and casting and show partial, discontinuous bonding along the meat, as can be seen in **Figure 16**. The UMo alloy in sets TL-05 and TL-06, as in sets TL-01 and TL-03, cracked; this is attributed to the very thin plate and the large reduction applied (68% total reduction).

4. Conclusions

The technique of encapsulation with low carbon steel was highly effective for the manufacture of thin foils of uranium and UMo alloy. During the rolling process, the texture of the crystalline plane (110) is induced; this anisotropy of the material affects its mechanical properties.

For both techniques, sputtering and TLPB applied for co-rolling of UMo alloy, its results are partially acceptable and the fragmentation of the UMo alloy occurs with total reduction over 45%, with foil thicknesses between 300 and 500 μm.

Acknowledgements

C. Marchant, E. Alcorta, and all the technical personal that are greatly acknowledged for their help in the support of this work.

References

[1] Snelgrove, J.L., Hofman, G.L., Meyer, M.K., Trybus, C.L. and Wiencek, T.C. (1997) Development of Very-High-

Density Low-Enriched-Uranium Fuels. *Nuclear Engineering and Design*, **178**, 119-126. http://dx.doi.org/10.1016/S0029-5493(97)00217-3

[2] Travelli, A. (1999) Presents of the RERTR Program in 1999. *Proceedings of the* 22*nd International Meeting on RERTR*, Budapest.

[3] Vatulin, A.V., Morozov, A.V., Suprun, V.B., Petrov, Yu.I. and Trifonov, Yu.I. (2004) High-Density U-Mo Fuel for Research Reactors. *Metal Science and Heat Treatment*, **46**, 484-489. http://dx.doi.org/10.1007/s11041-005-0007-5

[4] Parida, S.C., Dash, S., Singh, Z., Prasad, R. and Venugopal, V. (2001) Thermodynamic Studies on Uranium-Molybdenum Alloys. *Journal of Physics and Chemistry of Solids*, **62**, 585-597. http://dx.doi.org/10.1016/S0022-3697(00)00219-5

[5] Sinha, V.P., *et al.* (2009) Development, Preparation and Characterization of Uranium Molybdenum Alloys for Dispersion Fuel Application. *Journal of Alloys and Compounds*, **473**, 238-244. http://dx.doi.org/10.1016/j.jallcom.2008.05.061

[6] Kim, C.K., Park, J.M. and Ryu, H.J. (2007) Use of a Centrifugal Atomization Process in the Development of Research Reactor Fuel. *Nuclear Engineering and Technology*, **39**, 617-626. http://dx.doi.org/10.5516/NET.2007.39.5.617

[7] Keiser, D.D., Hayes, S.L., Meyer, M.K. and Clark, C.R. (2003) High-Density, Low-Enriched Uranium Fuel for Nuclear Research Reactors. *JOM*, **2003**, 55-58. http://dx.doi.org/10.1007/s11837-003-0031-0

[8] Soba, A. and Denis, A. (2007) An Interdiffusional Model for Prediction of the Interaction Layer Growth in the System Uranium-Molybdenum/Aluminium. *Journal of Nuclear Materials*, **360**, 231-241. http://dx.doi.org/10.1016/j.jnucmat.2006.09.014

[9] Meyer, M.K., Hofman, G.L., Hoyes, S.L., Clark, C.R., Wiencek, T.C., Snelgrove, J.L., Strain, R.V. and Kim, K.H. (2002) Low-Temperature Irradiation Behavior of Uranium-Molybdenum Alloy Dispersion Fuel. *Journal of Nuclear Materials*, **304**, 221-236. http://dx.doi.org/10.1016/S0022-3115(02)00850-4

[10] Lee, D.B., Kim, K.H. and Kim, C.K. (1997) Thermal Compatibility Studies of Unirradiated U-Mo Alloys Dispersed in Aluminum. *Journal of Nuclear Materials*, **250**, 79-82. http://dx.doi.org/10.1016/S0022-3115(97)00252-3

[11] Keisser Jr., D.D., Clark, C.R. and Meyer, M.K. (2004) Phase Development in Al-Rich U-Mo-Al Alloys. *Scripta Materialia*, **51**, 893-898. http://dx.doi.org/10.1016/j.scriptamat.2004.06.033

[12] Leenaers, A., Van den Berghe, S., Koonen, E., Jarousse, C., Huet, F., Trotabas, M., *et al.* (2004) Post-Irradiation Examination of Uranium-7 wt% Molybdenum Atomized Dispersion Fuel. *Journal of Nuclear Materials*, **335**, 39-47. http://dx.doi.org/10.1016/j.jnucmat.2004.07.004

[13] Ryu, H.J., Kim, Y.S., Hofman, G.L., Park, J.M. and Kim, C.K. (2006) Heats of Formation of (U, Mo)Al_3 and U(Al, Si)$_3$. *Journal of Nuclear Materials*, **358**, 52-56. http://dx.doi.org/10.1016/j.jnucmat.2006.06.013

[14] Lee, S.H., Park, J.M. and Kim, C.K. (2007) Thermophysical Properties of U-Mo/Al Alloy Dispersion Fuel Meats. *International Journal of Thermophysics*, **28**, 1578-1594. http://dx.doi.org/10.1007/s10765-007-0212-0

[15] Van den Berghe, S., Van Renterghem, W. and Leenaers, A. (2008) Transmission Electron Microscopy Investigation of Irradiated U-7 wt%Mo Dispersion Fuel. *Journal of Nuclear Materials*, **375**, 340-346. http://dx.doi.org/10.1016/j.jnucmat.2007.12.006

[16] Sinha, V.P., Hegde, P.V., Prasad, G.J., Dey, G.K. and Kamath, H.S. (2010) Effect of Molybdenum Addition on Metastability of Cubic γ-Uranium. *Journal of Alloys and Compounds*, **491**, 753-760. http://dx.doi.org/10.1016/j.jallcom.2009.11.060

[17] Clark, C.R., Hayes, S.L., Meyer, M.K., Hofman, G.L. and Snelgrove, J.L. (2004) Update on U-Mo Monolithic and Dispersion Fuel Development. *Transactions of the* 2004 *International Topical Meeting on Research Reactor Fuel Management*, Munich, 21-24 March 2004.

[18] Clark, C.R., Jue, J.F., Moore, G.A., Hallinan, N.P. and Park, B.H. (2006) Update on Monolithic Fuel Fabrication Methods. *Proceedings of the* 2006 *RERTR International Meeting*, Cape Town, 29 October-3 November 2006.

[19] Burkes, D.E., *et al*. (2007) Update on Mechanical Analysis of Monolithic Fuel Plates. *Proceedings of the Research Reactor Fuel Management Conference*, Lyon, 11-15 March 2007.

[20] Clark, C.R., *et al*. (2003) Monolithic Fuel Development at Argonne National laboratory. *Proceedings of the RERTR International Meeting*, Chicago, 5-10 October 2003.

[21] Sease, J.D., *et al*. (2007) Considerations in the Development of a Process to Manufacture Low-Enriched Uranium Foil Fuel for the High Flux Isotope Reactor. *Proceedings of the RERTR International Meeting*, Prague, 23-27 September 2007.

[22] Soba, A. and Denis, A. (2007) An Interdiffusional Model for Prediction of the Interaction Layer Growth in the System Uranium-Molybdenum/Aluminum. *Journal of Nuclear Materials*, **360**, 231-241. http://dx.doi.org/10.1016/j.jnucmat.2006.09.014

[23] Marin, J., *et al*. (2003) The Chilean LEU Fuel Fabrication Program. Status Report. *Proceedings of the RERTR International Meeting*, Chicago, 5-10 October 2003.

[24] Taub, J.M., Doll, D.T. and Hanks, G.S. (1958) Cold Working of Uranium. Los Alamos Scientific Laboratory, Los Alamos.

[25] Kim, K.H., Oh, S.J., Lee, D.B., Kim, C.K. and Sohn, D.S. (2006) Continuos Casting of Wide U-7% wt%Mo Alloy Foils for Monolithic Fuel by a Single Cooling Roll. *Proceedings of the Research Reactor Fuel Management Conference*, Sofia, 30 April-3 May 2006.

[26] Clark, C.R., Hallinan, N.P., Jue, J.F., Keiser, D.D. and Wight, J.M. (2006) Monolithic Fuel Fabrication Process Development. *Proceedings of the Research Reactor Fuel Management Conference*, Sofia, 30 April-3 May 2006.

[27] Moore, G.A., Jue, J.F. and Rabin, B.H. (2010) Full Size U-10Mo Monolithic Fuel Foil and Fuel Plate Fabrication-Technology Development. *Proceedings of the Research Reactor Fuel Management Conference*, Lisboa, 10-14 October 2010.

[28] Wyckoff, R.W.G. (1963) Uranium-Gamma. In: Wyckoff, R.W.G., Ed., *Crystal Structures I*, Second Edition, Interscience Publishers, New York, 7-83.

[29] Barrett, C.S. (1943) Structure of Metals: Crystallographic Method, Principles, and Data. McGraw-Hill Book Company, New York.

[30] Kocks, U.F. (2000) Texture and Anisotropy: Preferred Orientations in Polycrystalline and Their Effects on the Materials Properties. Cambridge University Press, Cambridge.

[31] Randle, V. and Engler, O. (2000) Introduction to Texture Analysis: Macrotexture, Microtexture and Orienting Mapping. CRC Press LLC, Boca Raton.

[32] Humphreys, F.J. and Hatherly, M. (2004) Recrystallization and Related Annealing Phenomena. Elsevier Science Ltd, Oxford.